A Methodology for Detecting Vessels in X-Ray Mammogram Images

Nick Cerneaz and Mike Brady
Robotics Research Group
Department of Engineering Science
Oxford University

Abstract: **Identification of the blood vessels and ıilk ducts within an X-ray mammogram image al-ɔws intelligent analysis of calcification clusters and ıass borders detected by other means. These vessel ɛatures are however generally buried within noise ·ith variance of the order of the vessel signal it-ɛlf. We present a scale-matched feature detector esigned to extract nominally 1-dimensional ridges ·om an image with a signal-to-noise ratio approxi-ıating unity. The algorithm uses first and second ifference gradient measures of the original non-noothed images to drive a search exploiting the *priori* knowledge of the expected vessel (ridge) fea-ıres. The algorithm is illustrated with an exam-le.**

1 Introduction

ɔreening of all women for breast cancer in the high risk ge groups of 50–65 years requires annual assessment three million X-ray films in the UK. Computerised ıalysis of a mammogram film can potentially improve ıe assessment of the film by giving the diagnostic ra-ologist additional information upon which to base a ɛcision.

In assessment of a mammogram film, it is desirable) be able to identify the vessels (both blood vessels ıd milk ducts, hereafter referred to simply as *vessels*) ithin a mammogram image. Some of the most im-ɔrtant mammographic indicators of breast cancer are ıked to their relative location and interaction with the ɛssels of the breast.

For instance, the degree of importance of a cluster of ılcifications (arguably the most important mammo-aphic indicator of cancer) is related to their localisa-ɔn within a single vessel, or their spread over a number adjacent vessels [Caseldine *et al.*, 1988]. The actual ɛtection of calcifications has been the subject of much fort and this issue is not addressed in this paper.

Another important mammographic indicator of de-loping tumours is a spiculated mass. The developing mour requires blood for survival and growth and ac-rdingly develops a series of blood vessels which "feed" e tumour. The vessels approach the tumour from all rections, resulting in a mammographic signature of central mass surrounded by a series of radial vessels, ther like the spokes of a bicycle wheel. In determining a potential mass is a spiculated mass it is important ɔt simply to assess the "roughness" of the mass bor-ɛr, but also to determine if the vessels approaching the ass *terminate* in the mass, or pass completely through e (2-D projected) mass [Caseldine *et al.*, 1988, ndolina *et al.*, 1992]. Knowledge of the vessel struc-ture in an image allows the assessment of vessel and mass interaction and the degree to which the vessels "feed" the masses.

Thus there is a range of diagnostic information than can be extracted from a mammogram image given knowledge of the corresponding vessel network. This paper briefly describes a system developed to extract the vessel network from a mammogram image. Section 2 describes the characteristics of the vessels and the images in which they are found, developing the constraints that the feature detector must accommodate. Section 3 looks at the traditional computer vision approaches to detecting features, identifying the shortcomings in relation to the present task. Section 4 initially states the vessel detector algorithm and then briefly reviews its components, while section 5 gives results of application of the algorithm to mammogram images.

2 Task Identification

When identifying the attributes of a successful vessel detector it is instructive to initially list the features of a vessel as presented in a typical digital image.

Imaged vessels present mammographically as regions of marginally lower film density (due to the increased X-ray beam attenuation due to the marginally higher material density along the X-ray path which traverses a vessel), and in the digitised image are thus of *higher* absolute grey-scale value. Thus we are interested in looking for nominally lighter regions against a darker background. A cursory glance at a mammogram image, for example that of figure 1(a), reveals that vessels are nominally 1-dimensional structures with low local curvature. By inspection, it is revealed that the absolute grey level difference between those pixels deemed by eye to belong to a vessel-like feature and those adjacent pixels that do not (the background) is often as low as $\sim 1.6\%$ of the available quantised intensity range (~ 4 intensity levels in an 8-bit quantisation). In Appendix A we show that the assumed gaussian image noise has variance $\sigma^2 \approx 1.2$–2% (3–5 grey levels at 8-bit resolution) of the intensity range, giving a signal-to-noise ratio (SNR) approximating unity in the worst case. There exists however, sufficient information to distinguish vessel pixels from background, since one can do it by eye. Clearly this information lies in the fact that the vessels are *connected*, and it is this structural information that separates the wheat from the chaff.

Unlike many typical industrial computer vision applications, the adjacent features (vessels) of these images may lie along side one another at a spacing of only a few pixels (given the digitisation resolution). Thus, in

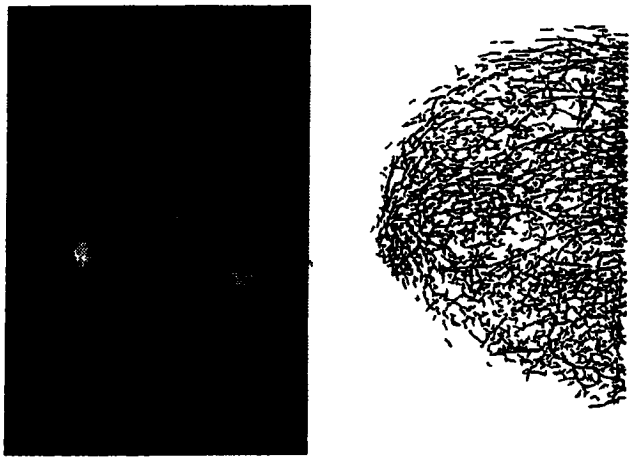

(a) Original image (b) "Vessels"

Figure 1: (a) A typical X-ray mammogram image. (b) The vessels identified by the algorithm presented in this paper.

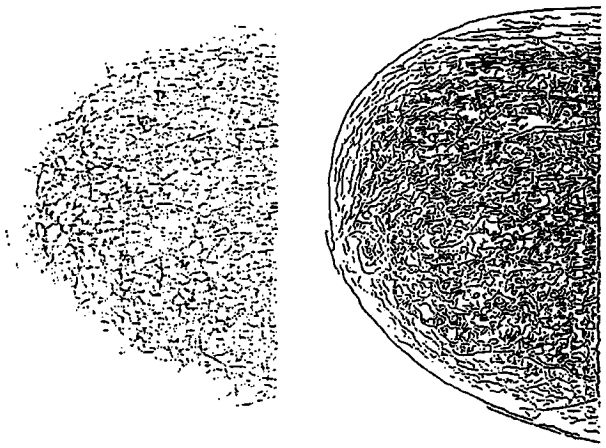

(a) Haralick ridges (b) Canny edges, $\sigma^2 = 1$

Figure 2: Results from general computer vision algorithms applied to the image of figure 1(a): (a) Haralick's ridge finder (b) Canny's edge detector.

combination with the low SNR, this means that any attempt to smooth an image (say, as a noise suppression technique) will either obliterate the signal, or merge adjacent vessels into larger features, altering the topology of the vessel network. Clearly, either effect is unacceptable.

Physiologically the majority of vessels range from capillaries up to $\sim$1–2mm diameters. The spatial extent of an imaged vessel in a direction perpendicular to its local axis is strictly dependent upon the digitisation resolution. We currently use mammogram images with a film resolution of 300μm square per pixel, meaning that most vessels will appear at widths up to $\sim$6 pixels.

In summary we require a system that can detect signals in unsmoothed images with SNR$\approx$1. The vessels present typically as nominally 1-dimensional structures at up to $\sim$6 pixels in width, with increased pixel intensity relative to the background or surrounding area that can be as low as 1.6% of the total intensity domain.

3 Traditional Computer Vision Techniques

Detection of edges and ridges in images has been the subject of widespread investigation in the computer vision community. All algorithms, at their simplest level, build a model of the feature to extract and look for existences of the model in the image. A vessel can be modelled (i) as a pair of back-to-back step transitions, or (ii) directly as an indivisible structure with a cross-section of a top-hat or a hump.

The first case is initially attractive because it suggests that conventional step/edge detectors followed by ridge finding using a logical combination of step pairs would be successful. In the case of mammogram images, many of the standard methods, such as Canny's gradient-based edge detector [1986], fail due to the low SNR and their need to pre-smooth the images, generally as a noise suppression technique. As an example of this, figure 2(b) shows the results of Canny's edge detector applied to the image of figure 1(a). Morphological edge detectors fare no better, a result that is tied directly to the structuring element, which cannot distinguish between noise and feature. Additional issues arise in the selection of the structuring element itself — is a spherical, ellipsoidal or other element best suited to the expected edge profile?

A. Determine the second difference responses in a number of directions.

B. At each pixel, combine the information from the second differences calculated in the various directions, segmenting the image into pixels with significant positive, significant negative, or insignificant response.

C. Correct for errors due to noise and other artifacts.

D. Hypothesise boundary locations that explain the observed second difference response patterns.

Figure 3: The broad philosophy behind Fleck's *Phantom* edge detector and the algorithm presented in the present work.

The second case, of directly modelling a ridge has been the subject of little attention in the computer vision literature since attempts to generalise the model of a ridge in order to develop an algorithm leave it oversimplified and incapable of capturing the peculiarities of most practical applications. Consequently most successful implementations are application specific. An example of a general ridge finder is the ridge/ravine finder of Haralick [1992] based on the bicubic facet model. The results of applying this method to the image of figure 1(a) are shown in figure 2(a). The poor response is mostly attributable to the low SNR. Clearly these general methods are inappropriate for the present task.

Fleck [1988] describes an edge finder system, named *Phantom*, based on topological interpretation of second difference measures of an unsmoothed image. In the broadest generalisation possible, the *Phantom* edge finding process can be summarised as in figure 3.

The secret to *Phantom*'s success lies in the details

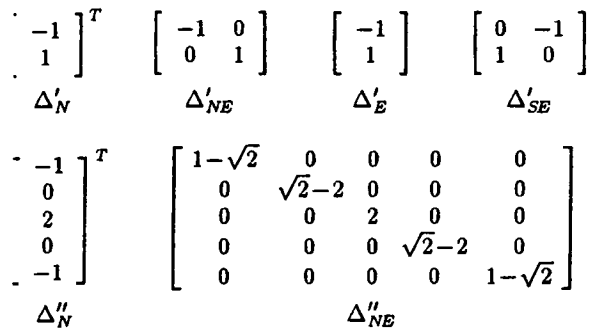

igure 4: The difference operators Δ' and Δ''. Note iat $[\Delta''_E] = [\Delta''_N]^T$ and $[\Delta''_{SE}]$ is formed by mirror fold- ig $[\Delta''_{NE}]$ about its central column. The results of the .' convolution are assigned to the pixel at the top left)rner of the mask, whilst the Δ'' result is assigned to ie central pixel of the mask.

' the algorithms to combine the directional informa- on and suppress the errors. By combining both shape id amplitude information into a single summation over ie *maximal star-convex* neighbourhood surrounding ich pixel[1], the algorithm can distinguish real responses om those due to noise. It is within this framework of)isy feature detection and subsequent noise suppres- on based on careful interpretation of the data that the 'esent work is grounded.

4 The Mammogram Vessel Detector

the first instance the framework of the algorithm is mply stated and this is followed by a brief discussion it's composition.

1 *The Ridge/Vessel Detector Algorithm*

:t Δ'_α and Δ''_α be the first and second difference fil- rs respectively, where $\alpha = \{N, NE, E, SE\}$ represent- g the north, north-east, east and south-east directions spectively (see figure 4). Let the convolution of these ters with the image I be represented as $I'_\alpha = \Delta'_\alpha * I$, id $I''_\alpha = \Delta''_\alpha * I$. Let $I(i,j)$, $I'_\alpha(i,j)$ and $I''_\alpha(i,j)$ be the iage value at the pixel with coordinates (i,j) of the spective image. Using this notation, the algorithm is us:

Form the eight difference images I'_α and I''_α.

Find the gradient of the image surface, ∇I, using the first difference images I'_α. Since the image I is not pre-smoothed before calculating I'_α and the spatial extent of the Δ' filters is so small (2 pixels), there are numerous local errors in I'_α that deem the simple summation at each pixel of the appropriate I'_α components of ∇I susceptible to unknown corruption. It is therefore necessary to consider the available evidence for an image gradient at each pixel.

[1]Within the scope of Fleck's definition, the maximal star- nvex neighbourhood surrounding a pixel is that region thin a given fixed radius from the pixel that maintains :onstant sign of the second difference response, ensuring at each point of the region can be connected to the pixel a straight path contained entirely within the region.

At each pixel (i,j) in I, take the eight I'_α values that involve the pixel in their calculation and form the vectors

$$\mathbf{H} = \begin{bmatrix} I'_N(i,j) \oplus I'_N(i-1,j) \\ I'_E(i,j) \oplus I'_E(i,j-1) \end{bmatrix}$$

$$\mathbf{D} = \begin{bmatrix} I'_{NE}(i,j) \oplus I'_{NE}(i-1,j-1) \\ I'_{SE}(i-1,j) \oplus I'_{SE}(i,j-1) \end{bmatrix}$$

where the coordinate system of $\mathbf{D}$ is that of $\mathbf{H}$ rotated through $\frac{\pi}{4}$ radians, the $\oplus$ operator returns the maximal response of the two arguments such that if they are of the same sign then return the algebraic sum of the arguments, otherwise return the argument with the maximum absolute value.

If a consistent gradient vector occurs over the neighbourhood of the pixel, then the vectors $\mathbf{H}$ and $\mathbf{D}$ should be roughly aligned (with $\mathbf{D}$ expressed in the coordinate system of $\mathbf{H}$). Thus if the included angle is below some threshold, then there is consistent evidence across the neighbourhood for the existence of the image gradient, and it is thus set[2]:

$$\nabla I(i,j) = \begin{cases} \mathbf{H} + \mathbf{D} & \text{if } \arg(\mathbf{H}) - \arg(\mathbf{D}) < \theta_{\Delta'} \\ \mathbf{0} & \text{otherwise.} \end{cases}$$

3. Select *all* pixels with a significant Δ'' response as feature candidates by forming the set $\mathbf{N}$ as[3]:

$$\mathbf{N} = \Big\{(i,j) : \max\Big(I''_N(i,j), I''_{NE}(i,j), I''_E(i,j), I''_{SE}(i,j)\Big) > T_{\Delta''}\Big\}$$

4. Scan the set $\mathbf{N}$, omitting any pixels that form 8-connected regions of fewer than a given number of pixels.
5. Take the remaining 8-connected regions of set $\mathbf{N}$ and thin them down to a simply connected *skeleton* that is approximately on the medial-axis of the regions. Form the set $\mathbf{S}$ of pixels lying on these region skeletons.
6. Track along the elements of set $\mathbf{S}$ linking together into *bones* $\mathbf{b}$ those elements that lie in the same direction. Upon encountering a branch in the skeleton, initiate another bone. Continue classifying the elements of set $\mathbf{S}$ until no further unclassified elements remain. Reject those bones of insufficient length, forming the set $\mathbf{B}$ of all retained bones $\mathbf{b}$.
7. Follow the axis/skeleton of each bone $\mathbf{b} \in \mathbf{B}$. Searching in a direction perpendicular to the local axis (heading), search the set $\mathbf{N}$ for 8-connected pixels

[2]The threshold $\theta_{\Delta'}$ is normally set to a high value, say $\theta_{\Delta'} \approx \frac{\pi}{2}$ to allow for the variation due to the noise. Note that this threshold does not effect the value of the image gradient calculated at (i,j), rather it defines the point at which the available evidence for an image gradient is, or is not believed.

[3]In the current implementation the threshold $T_{\Delta''}$ is set *at each pixel* (i,j) to a percentage of the variance of all I''_α values where α is the direction in which the max(...) occurs. Typically this threshold is set to $T_{\Delta''} \approx$70–80% of the standard deviation σ.

that surround the skeleton pixels of bone **b**. Observing the image gradients calculated at step 2 retain in the *vessel* **v** those pixels that do not contradict the notion of a vessel with the local heading of **b**. Initiate a new vessel **v** for each bone of set **B** encountered, and continue until **B** is exhausted.

8. Declare the set of all vessels **v** to be the "vessels" of the image I.

4.2 The Algorithm Briefly Reviewed

Since the vessels are of higher intensity and are typically up to ~6pixels in widths, the second difference operators Δ'' of figure 4 (which are actually scaled, inverted second difference operators) with spatial extent of 5 pixels were chosen to match the spatial characteristics of the expected vessel profile, rather than for the general computer vision reasons of image interlacing (which is not present in these images due to the digitisation process). Step 3 (which equates to step B of figure 3) collects only those pixels that are potential/candidate vessel pixels, whilst steps 4–8 introduce knowledge of the expected vessel profile to rule out artifacts (steps C and D of figure 3). It is in these steps that the direct modelling of the vessel profile is introduced into the system.

The exact details of the various implementations (eg. the thinning algorithm of step 5) are superfluous to the methodology presented in section 4.1 and are omitted for simplicity.

5 Results

Although it is somewhat difficult to present quantitative results, for completeness the result of running the algorithm over the image of figure 1(a) is given in figure 1(b). Similar results are obtained for images digitised across a variety of platforms. The strength of this algorithm is that the feature description allows many other tasks to be undertaken. For example, "removing" the vessels gives an image freed from the textural clutter of the vessels, allowing improved detection and analysis of masses, and improved tissue classification. Combining calcification data with the vessel description (mainly the local vessel direction) improves differentiation between arterial/venous calcifications and ductal calcifications.

6 Conclusion

We present the framework of an implemented algorithm for extracting a description of the vessel features from X-ray mammogram images. The algorithm is scale-space matched to the expected cross-section of the vessels, and whilst the algorithm has not been implemented at varying scales, there is no reason why this could not be done. The algorithm can successfully differentiate spatially adjacent features, and resolve features with a SNR approximating unity.

Current work is directed towards developing clinically significant tools using the vessel description to analyse calcification clusters, masses (in particular spiculated masses) and bilateral asymmetry using both the vessel networks themselves and the texturally less cluttered "removed-vessel" images for comparison.

A Feature Signal-to-Noise

Digital X-ray mammogram images are typically attained by digitising X-ray film mammograms (although the technology exists for direct digital imaging, this is not likely to make a significant clinical impact for some time). The digitisation process itself introduces white gaussian noise, predominantly shot noise within the imaging device, in addition to any noise introduced during the X-ray exposure/developing of the mammogram film.

In order to determine the average noise level of an image, consider the *facet-based peak noise* model of Haralick [Haralick and Shapiro, 1992]. Following Haralick, fit a sloped facet approximation to the image surface, and determine the squared differences between the fitted surface and the image as:

$$\epsilon^2_{(i,j)} = \sum_{(r,c)\in N} \left[\hat{\alpha}r + \hat{\beta}c + \hat{\gamma} - I(r,c)\right]^2$$

where N is the 8-connected region over (r,c) surrounding the central pixel (i,j) over which the facet-model is fitted to the data, and I is the raw image data. A least-squares minimisation of ϵ^2 gives the model parameters $\hat{\alpha}$, $\hat{\beta}$ and $\hat{\gamma}$ at each (i,j). Each neighbourhood's normalised squared residual error $\epsilon^2/(\sum_r \sum_c 1 - 3)$ can constitute an unbiased estimator for the variance σ^2 of the noise. When averaged over all the pixels in an image this is a stable estimator of σ^2. In the present example, this estimator is further stabilised by only calculating ϵ^2 over neighbourhoods consisting entirely of background pixels, since the sloped-facet model in addition to assuming a gaussian noise process also assumes that the underlying *real* image surface is a piecewise linear surface over the pixel neighbourhood. This assumption finds more support in background regions.

Implementation of this method over many images of varying conditions and digitisation processes shows that the background noise is of zero mean and variance $\sigma^2 \approx$ 3–5 intensity levels.

Acknowledgements

NC acknowledges the support of the Rhodes Trust.

References

[Andolina *et al.*, 1992] V.F. Andolina, S.L. Lillé, and K.M. Willison. *Mammographic Imaging.* J. B. Lippincott Company, Philadelphia, 1992.

[Canny, 1986] J. Canny. A computational approach to edge detection. *IEEE PAMI*, 8(6):679–698, 1986.

[Caseldine *et al.*, 1988] J. Caseldine, R. Blamey, E. Roebuck, and C. Elston. *Breast Disease for Radiographers.* Wright, London, 1988.

[Fleck, 1988] M.M. Fleck. Boundaries and Topological Algorithms. PhD Thesis. Technical Report 1065, MIT Artificial Intelligence Laboratory, 1988.

[Haralick and Shapiro, 1992] R.M. Haralick and L.G. Shapiro. *Computer & Robot Vision, Vol 1.* Addison-Wesley Publishing, Reading, Mass., 1992.